Materials Advances

ROYAL SOCIETY OF CHEMISTRY

COMMUNICATION

View Article Online
View Journal | View Issue

Check for updates

Cite this: *Mater. Adv.*, 2022, 3, 6446

Received 12th April 2022,
Accepted 7th June 2022

DOI: 10.1039/d2ma00413e

rsc.li/materials-advances

Evaluating the thermal behaviour of benzimidazolylidene sources for thin-film applications†

Alex J. Veinot, ‡[a] Matthew B. E. Griffiths, ‡[b] Ishwar Singh, [a] Joseph A. Zurakowski,[b] Paul A. Lummis, [a] Seán T. Barry *[b] and Cathleen M. Crudden *[ac]

We show that the N-heterocyclic carbene precursor employed has a significant influence on the purity of the resulting films prepared by vapour-phase deposition. 1,3-Diisopropylbenzimidazolylidene is stable up to 363 K, before undergoing thermal decomposition to 1,2-diisopropylbenzimidazole as the major product. Various minor products arising from wing-tip loss are also observed. Kinetic and thermochemical analyses indicate that this reaction is second-order with respect to the carbene and proceeds through a transient tetraazafulvalene.

N-Heterocyclic carbenes (NHCs, **I**) are an important class of ligands in molecular chemistry with emerging applications in materials chemistry.[1] As exceptional σ-donors, NHCs are capable of binding strongly to gold and other metal surfaces and the resulting monolayers possess high chemical and thermal stability.[2] Self-assembled monolayers (SAMs) of NHCs have been formed on Cu,[3] Au,[1,2] Ag,[3a] Pt,[4] and Mg surfaces,[5] and have shown promise in applications such as biosensing,[6] surface patterning,[7] and metal oxide etching.[8] Among NHC SAMs published to date, 1,3-diisopropylbenzimidazolylidene (benzNHC^{iPr}) has received considerable attention. Flanking isopropyl groups (wing-tip groups) reinforce an upright binding mode and promote long-range order,[9] essential properties for NHC SAMs to be effective in material science applications.

Vapour deposition methods are commonly used to prepare NHC monolayers and overlayers, and enable the use of ultra-high vacuum (UHV) surface science analytics.[3,4a,8,10a] Furthermore, vapour-phase deposition can be advantageous for high-volume manufacturing (HVM) applications since it removes the need to recycle or replace a solvent system, leading to lower production costs and environmental impact.

While preparing these films, the free NHC **I** can be employed after preparation *via* deprotonation of the salt **II**, but is more commonly generated *in situ* thermally from either carboxylate **III** or hydrogen carbonate salt **IV** (Scheme 1).[10] It is generally

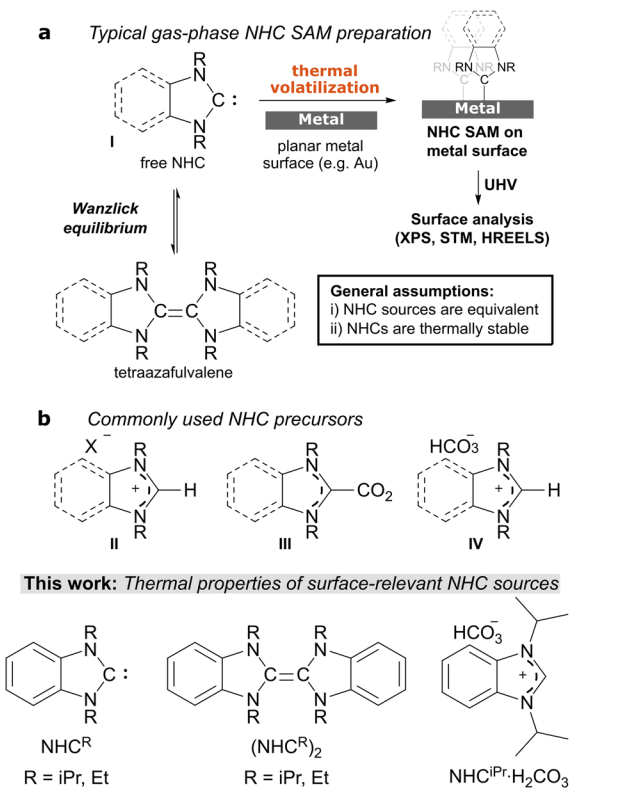

Scheme 1 (a) Typical workflow for studying NHC SAMs on metallic surfaces. (b) Common and surface-relevant NHC precursors and NHC sources examined here.

[a] *Department of Chemistry, Queen's University, 90 Bader Lane, Kingston, Ontario, K7L 3N6, Canada*
[b] *Department of Chemistry, Carleton University, 1125 Colonel By Drive, K1S 5B6, Ottawa, Ontario, Canada*
[c] *Institute of Transformative Bio-Molecules, ITbM-WPI, Nagoya University, Nagoya, Chikusa, 464-8601, Japan*

† Electronic supplementary information (ESI) available: Experimental, spectroscopic, and crystallographic details for CCDC 2151982 and 2151983. For ESI and crystallographic data in CIF or other electronic format see DOI: https://doi.org/10.1039/d2ma00413e

‡ These authors contributed equally.

assumed that differences between NHC sources are minimal such that the resulting SAMs formed during volatilisation are equivalent. While preparing NHC overlayers with benzNHC^{iPr} and its precursor hydrogen carbonate salt benzNHC^{iPr}·H_2CO_3, it became apparent from X-ray photoelectron spectroscopy (XPS) that this was not true, prompting us to study the thermochemistry of several important NHC SAM precursors by thermogravimetric analysis (TGA). Herein, we provide a comprehensive thermochemical study on benzNHC^{iPr}, its precursor hydrogen carbonate salt benzNHC^{iPr}·H_2CO_3 and the related tetraazafulvalene (benzNHC^{Et})$_2$. The results shed light on optimal precursor choice, decomposition products, likely mechanisms of decomposition and the effect of decomposition products on surface analysis.

Carbene benzNHC^{iPr} was prepared following a known literature procedure,[11] and purified by vacuum distillation to remove trace iodide contaminants. To examine films prepared from the free carbene, neat benzNHC^{iPr} prepared and purified as above was sublimed at 373 K onto a copper wafer. Decomposition of the residual NHC (distillant) was evident from a colour change to orange from colourless, and from ^{1}H NMR spectroscopic analysis. Analysis of the resulting NHC-modified copper surface using XPS indicated that although a benzNHC^{iPr} overlayer was present, decomposition products were also transferred to the copper surface, evident by a broad peak with bimodal distribution in the N 1s region (Fig. 1b). This prompted further study of the thermal stability of the isolated carbene benzNHC^{iPr}.

To gain further insights, we carried out a bulk thermolysis reaction of benzNHC^{iPr}. Using a sand bath heated between 453–483 K, neat benzNHC^{iPr} was thermolysed over 4 h in a sealed vessel (Scheme 2). The resulting dark brown-coloured oil was purified by column chromatography, yielding 1,2-diisopropylbenzimidazole (39%, **1a**) and 1-isopropyl-benzimidazole (21%, **1b**) as the major and minor products, respectively. The structures of benzNHC^{iPr} and **1a** were determined using single crystal X-ray diffraction (Scheme 2, see ESI† for details). Benzimidazole **1a** is a structural isomer of benzNHC^{iPr} and was also characterised using ^{1}H and ^{13}C {^{1}H} NMR spectroscopy and elemental analysis (see ESI†). Benzimidazole **1b** has been previously described,[11] arising from the loss of a wing-tip group from benzNHC^{iPr}. Its structure was verified using ^{1}H NMR spectroscopy.

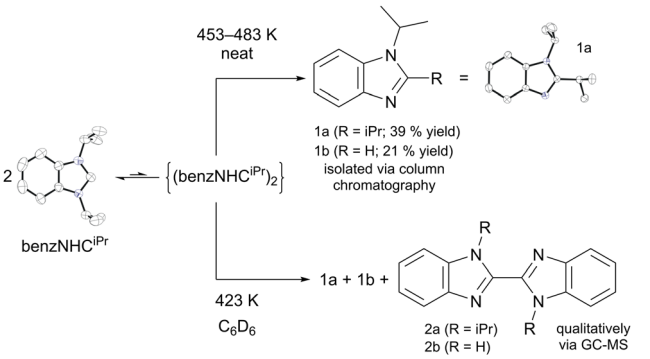

Scheme 2 Proposed thermal decomposition of benzNHC^{iPr} through its transient tetraazafulvalene. For full crystallographic details, see ESI.†

The thermolysis reaction of benzNHC^{iPr} was repeated in a C_6D_6 solution at 423 K, and subsequent qualitative analysis using GC-MS revealed that in addition to **1a** and **1b**, 2,2′-bibenzimidazoles **2a** and **2b** are produced. Lappert and coworkers previously demonstrated the conversion of 1,2-dibenzylbenzimidazole to bibenzimidazoles,[12a] so **1a** was examined by TGA to test for further decomposition (Fig. 3a).

Using a 10 mM 1,2-dichloroethane solution, **1a** was deposited onto a copper surface and studied using XPS. In the N 1s XPS region, **1a** exhibits two peaks each fit using a single component at 399.4 eV and 400.9 eV for amine and imine moieties, respectively (Fig. 1c). These peaks are similar in binding energy to the ones observed from vapor deposition of benzNHC^{iPr}, suggesting that benzimidazole contaminants likely co-deposited with free NHC. Due to overlap in the N 1s binding energies for organic compounds, benzimidazole **1b** or 2,2′-bibenzimidazoles **2a** and **2b** cannot be discounted as surface contaminants and will be indistinguishable in these studies.

Similar decomposition reactions are known for NHCs and their heteroatom congeners bearing allyl, imino and benzyl wing-tip groups.[12] Radicals and tetraazafulvalenes (or related carbene dimers) have been implicated in these rearrangements, the latter accessible *via* the Wanzlick equilibrium.[13] The dimerisation of benzimidazolylidenes is highly sensitive to the steric properties of the wing-tip substituents,[14] such that formation of (benzNHC^{iPr})$_2$ is unexpected.[14c]

Evidence for the formation of (benzNHC^{iPr})$_2$ during thermal decomposition was provided by solution-phase kinetics measurements in C_6D_6 between 423–453 K (Scheme 2, see ESI† for details). The concentration of benzNHC^{iPr} was monitored by ^{1}H NMR spectroscopy and examined using first, second and third-order integrated rate laws. Both second-order (Fig. 2a) and third-order (Fig. S10, ESI†) rate laws yielded linear relationships, suggesting a complicated thermal mechanism. While

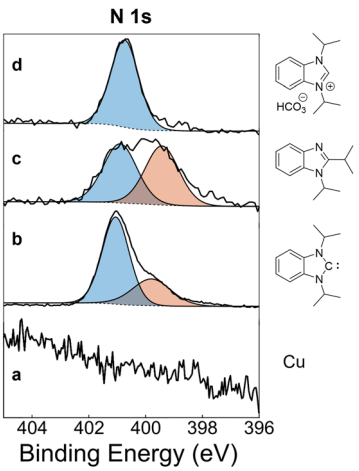

Fig. 1 N 1s XPS studies for (a) a cleaned copper surface, (b) a copper surface treated with sublimed benzNHC^{iPr} (373 K), (c) a copper surface treated with 10 mM solution of **1a** in 1,2-dichloroethane, and (d) a copper surface treated with sublimed benzNHC^{iPr}·H_2CO_3 (373 K).

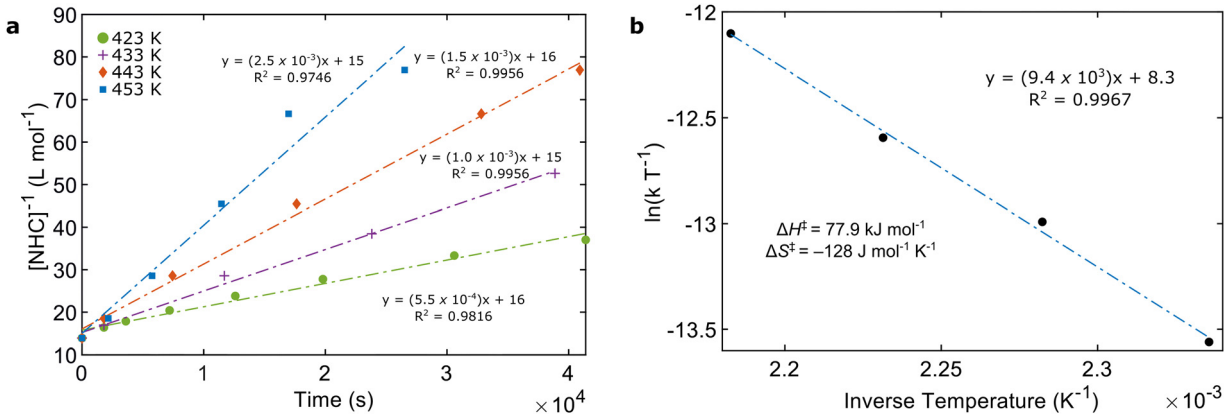

Fig. 2 (a) Summary of kinetic measurements performed for benzNHC^{iPr} (423–453 K) in C_6D_6 (sealed NMR tube, 0.072 M benzNHC^{iPr}, 0.086 M toluene as an internal standard). (b) Eyring–Polanyi plot derived from the kinetics measurements in (a); $\Delta H^{\ddagger}$ and $\Delta S^{\ddagger}$ were derived from the slope and intercept of the linear regression, respectively.

trimolecular reactions are uncommon, our data may indicate the establishment of a monomer/dimer pre-equilibrium during thermal decomposition.[14d,e] Assuming that the rate-determining transition state is bimolecular with respect to benzNHC^{iPr}, an Eyring–Polanyi plot (Fig. 2b) yields the activation enthalpy ($\Delta H^{\ddagger}$ = 77.9 kJ mol^{-1}) and entropy ($\Delta S^{\ddagger}$ = −128 J mol^{-1} K^{-1}). For comparison, the enthalpy (ΔH°) and entropy (ΔS°) of dissociation for the equilibrium between benzNHC^{Et} and its dimer are 57.3 kJ mol^{-1} and 127 kJ mol^{-1} K^{-1}, respectively.[14b] Compared to the dimerisation of benzNHC^{Et}, the sign and magnitude of $\Delta S^{\ddagger}$ supports the formation of (benzNHC^{iPr})$_2$ during thermal decomposition while sterically larger iPr groups increase $\Delta H^{\ddagger}$ and suppress dimerisation.

Since (benzNHC^{iPr})$_2$ is fleeting and could not be isolated, (benzNHC^{Et})$_2$ was prepared instead and studied using TGA (Fig. 3a).[14b] For (benzNHC^{Et})$_2$, an onset of mass loss occurs around 453 K, which is 130 K higher than benzNHC^{iPr} and is a consequence of increased molecular weight upon dimerisation. An inflection was observed around 493 K, which is likely related to the conversion of (benzNHC^{Et})$_2$ to its monomer.[14b]

For comparison, the thermogram of benzNHC^{iPr} (Fig. 3b) shows an onset of mass loss at 323 K (**i**), coincident with the melting point of benzNHC^{iPr} (322 K) determined using differential scanning calorimetry (DSC) (point a, yellow region). At 453 K, an inflection is observed (**ii**) which can be attributed to sample volatilisation. However, DSC measurements indicate that decomposition begins around 363 K (point b, purple region), culminating in a major exothermic event around 453 K (point c, red region), coincident with the observed inflection point **ii** from TGA, suggesting that volatilisation and decomposition occur over a similar temperature regime. A second thermal inflection is found at 483 K in the DSC curve (point d, green region), suggesting that an ongoing, complicated thermal decomposition continues as the temperature is increased. Using neat samples of benzNHC^{iPr} and (benzNHC^{Et})$_2$, a thermal scrambling experiment was completed using our thermolysis conditions. The mixture of products

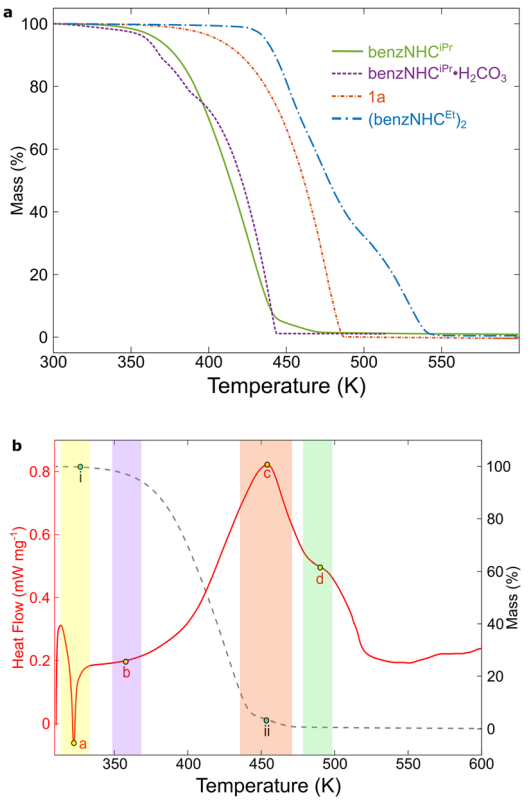

Fig. 3 (a) Stack TGA plot for benzNHC^{iPr} (green), benzNHC^{iPr}·H_2CO_3 (violet), **1a** (orange) and (benzNHC^{Et})$_2$ (blue); Ramp: 10 °C min^{-1}, Mass loading: 10 ± 2 mg, (b) TGA (grey) and DSC (red) curves for benzNHC^{iPr}. Areas of interest shown in coloured bars.

obtained could not be resolved by ^{1}H NMR spectroscopy; however, cross-over products containing both ethyl and isopropyl wing-tips were detected by ESI-MS (see ESI†) providing further qualitative evidence that the thermolysis of NHC proceeds bimolecularly.

As an alternative to often air-sensitive free carbenes, azolium hydrogen carbonate salts have been used as effective, air-stable precursors for vapour phase depositions of NHCs onto Cu, Au

and Pt surfaces.[3b,4a,15] When heated, these salts liberate H_2O and CO_2, generating free NHCs in the process (eqn (1)).[16] To examine the preparation of NHC overlayers with this precursor, we heated benzNHC^{iPr}·H_2CO_3 to 373 K in the presence of a copper wafer. The successful formation of an NHC overlayer was indicated by a single symmetric peak in the N 1s XPS region, fit using one component centred at 400.7 eV (Fig. 1d). XPS analysis indicated that films prepared using benzNHC^{iPr}·H_2CO_3 had a clean monomodal distribution in the N 1s region, unlike the bimodal distribution for free benzNHC^{iPr}.

$$\text{benzNHC}^{iPr} \cdot H_2CO_3 \xrightarrow{\Delta} \text{benzNHC}^{iPr} + H_2O + CO_2 \qquad (1)$$

TGA was performed for benzNHC^{iPr}·H_2CO_3 to understand these differences (Fig. 3a, purple). The thermogram shows that water and carbon dioxide are lost by 395 K indicating the *in situ* formation of free benzNHC^{iPr}.[16a]

With increasing temperature, a smooth exponential decay to zero residual mass was observed, consistent with clean volatilisation, unlike free benzNHC^{iPr}, which has an inflection before coming to zero residual mass. The thermogram of benzNHC^{iPr}·H_2CO_3 was insensitive to heating rate or added KI, the latter a possible contaminant in benzNHC^{iPr} arising from its preparation. Co-mixing benzNHC^{iPr}·HI and benzNHC^{iPr}·H_2CO_3 produced a similar curve as those found in the literature,[16b] suggesting that incomplete anion exchange may have occurred in previous studies. Co-mixing of benzNHC^{iPr}·HI and benzNHC^{iPr}·H_2CO_3 also reproduced the TGA inflection observed for free benzNHC^{iPr}, suggesting possible acid-catalysis involved in the decomposition (see ESI†).[14d,e] Since the thermolysis of benzNHC^{iPr} is likely bimolecular, differences in thermal behaviour between benzNHC^{iPr} and benzNHC^{iPr}·H_2CO_3 likely arise from the kinetics of the release of carbene. The use of benzNHC^{iPr}·H_2CO_3 in NHC generation results in a lower flux of benzNHC^{iPr} at any given time, which minimises thermal decomposition.

In summary, TGA and DSC measurements have shown that benzNHC^{iPr} thermally decomposes during volatilisation above 363 K. This reaction proceeds through the transient tetraazafulvalene (benzNHC^{iPr})$_2$ to primarily afford benzimidazoles **1** and **2**. Analysis of N 1s XPS suggests that these decomposition products can persist on copper surfaces and complicate peak fitting. These impurities were not observed in films prepared under similar conditions using benzNHC^{iPr}·H_2CO_3, illustrating that selecting the right NHC source is an important consideration for thermal applications. As on-surface applications of NHCs are being rapidly discovered, detailed thermochemical analyses of NHCs have become a necessary part of the toolkit for proper qualitative and quantitative surface analysis.

Conflicts of interest

There are no conflicts to declare.

Acknowledgements

The Natural Sciences and Engineering Research Council of Canada (NSERC) and the Canada Foundation for Innovation (CFI) are thanked for support of this work in terms of operating and equipment grants to C. M. C. and S. T. B. (RGPIN-2019-06213). NSERC is also thanked for a Vanier Scholarship (A. J. V), a CGS-D scholarship to M. B. E. G., and an Undergraduate Student Research Award (J. A. Z.). I. S. acknowledges Queen's University for the RT Mohan Scholarship and the Ontario government for a Graduate Scholarship.

Notes and references

1 (*a*) H. V. Huynh, *Chem. Rev.*, 2018, **118**, 9457; (*b*) M. N. Hopkinson, C. Richter, M. Schedler and F. Glorius, *Nature*, 2014, **510**, 485; (*c*) C. A. Smith, M. R. Narouz, P. A. Lummis, I. Singh, A. Nazemi, C.-H. Li and C. M. Crudden, *Chem. Rev.*, 2019, **119**, 4986; (*d*) S. Engel, E.-C. Fritz and B. J. Ravoo, *Chem. Soc. Rev.*, 2017, **46**, 2057; (*e*) A. V. Zhukhovitskiy, M. J. MacLeod and J. A. Johnson, *Chem. Rev.*, 2015, **115**, 11503; (*f*) T. Weidner, J. E. Baio, A. Mundstock, C. Große, S. Karthäuser, C. Bruhn and U. Siemeling, *Aust. J. Chem.*, 2011, **64**, 1177; (*g*) A. V. Zhukhovitskiy, M. G. Mavros, T. Van Voorhis and J. A. Johnson, *J. Am. Chem. Soc.*, 2013, **135**, 7418.

2 C. M. Crudden, J. H. Horton, I. I. Ebralidze, O. V. Zenkina, A. B. McLean, B. Drevniok, Z. She, H.-B. Kraatz, N. J. Mosey, T. Seki, E. C. Keske, J. D. Leake, A. Rousina-Webb and G. Wu, *Nat. Chem.*, 2014, **6**, 409.

3 (*a*) L. Jiang, B. Zhang, G. Médard, A. P. Seitsonen, F. Haag, F. Allegretti, J. Reichert, B. Kuster, J. V. Barth and A. C. Papageorgiou, *Chem. Sci.*, 2017, **8**, 8301; (*b*) C. R. Larrea, C. J. Baddeley, M. R. Narouz, N. J. Mosey, J. H. Horton and C. M. Crudden, *Chem. Phys. Chem.*, 2017, **18**, 3536.

4 (*a*) Y. Zeng, T. Zhang, M. R. Narouz, C. M. Crudden and P. H. McBreen, *Chem. Commun.*, 2018, **54**, 12527; (*b*) S. Dery, S. Kim, G. Tomaschun, T. Berg, D. Feferman, A. Cossaro, A. Verdini, D. Floreano, T. Klüner, F. D. Toste and E. Gross, *J. Phys. Chem. Lett.*, 2019, **10**, 5099.

5 L. Stephens, J. D. Padmos, M. R. Narouz, A. Al-Rashed, C.-H. Li, N. Payne, M. Zamora, C. M. Crudden, J. Mauzeroll and J. H. Horton, *J. Electrochem. Soc.*, 2018, **165**, G139.

6 C. M. Crudden, J. H. Horton, M. R. Narouz, Z. Li, C. A. Smith, K. Munro, C. J. Baddeley, C. R. Larrea, B. Drevniok and B. Thanabalasingam, *Nat. Commun.*, 2016, **7**, 12654.

7 (*a*) D. T. Nguyen, M. Freitag, M. Körsgen, S. Lamping, A. Rühling, A. H. Schaefer, M. H. Siekman, H. F. Arlinghaus, W. G. van der Wiel and F. Glorius, *Angew. Chem., Int. Ed.*, 2018, **57**, 11465; (*b*) Z. She, M. R. Narouz, C. A. Smith, A. MacLean, H.-P. Loock, H.-B. Kraatz and C. M. Crudden, *Chem. Commun.*, 2020, **56**, 1275.

8 A. J. Veinot, A. Al-Rashed, J. D. Padmos, I. Singh, D. S. Lee, M. R. Narouz, P. A. Lummis, C. J. Baddeley, C. M. Crudden and J. H. Horton, *Chem. – Eur. J.*, 2020, **26**, 11431.

9 (*a*) A. Inayeh, R. R. K. Groome, I. Singh, A. J. Veinot, F. Crasto de Lima, R. H. Miwa, C. M. Crudden and A. B. McLean, *Nat.*

Commun., 2021, **12**, 4034; (*b*) G. Lovat, E. A. Doud, D. Lu, G. Kladnik, M. S. Inkpen, M. L. Steigerwald, D. Cvetko, M. S. Hybertsen, A. Morgante, X. Roy and L. Venkataraman, *Chem. Sci.*, 2019, **10**, 930.

10 (*a*) G. Wang, A. Rühling, S. Amirjalayer, M. Knor, J. B. Ernst, C. Richter, H.-J. Gao, A. Timmer, H.-Y. Gao, N. L. Doltsinis, F. Glorius and H. Fuchs, *Nat. Chem.*, 2017, **9**, 152; (*b*) L. Delaude, *Eur. J. Inorg. Chem.*, 2009, 1681.

11 O. Starikova, G. Dolgushin, L. Larina, T. Komarova and V. Lopyrev, *ARKIVOC*, 2003, **13**, 119.

12 (*a*) B. Çetinkaya, E. Çetinkaya, J. A. Chamizo, P. B. Hitchcock, H. A. Jasim, H. Küçükbay and M. F. Lappert, *J. Chem. Soc., Perkin Trans. 1*, 1998, 2047; (*b*) C. Holtgrewe, C. Diedrich, T. Pape, S. Grimme and F. E. Hahn, *Eur. J. Org. Chem.*, 2006, 3116; (*c*) G. Steiner, A. Krajete, H. Kopacka, K.-H. Ongania, K. Wurst, P. Preishuber-Pflügl and B. Bildstein, *Eur. J. Inorg. Chem.*, 2004, 2827.

13 (*a*) M. K. Denk, K. Hatano and M. Ma, *Tetrahedron Lett.*, 1999, **40**, 2057; (*b*) H. W. Wanzlick, *Angew. Chem., Int. Ed. Engl.*, 1962, **1**, 75.

14 (*a*) F. E. Hahn, L. Wittenbecher, D. Le Van and R. Fröhlich, *Angew. Chem., Int. Ed.*, 2000, **39**, 541; (*b*) Y. Liu, P. E. Lindner and D. M. Lemal, *J. Am. Chem. Soc.*, 1999, **121**, 10626; (*c*) W. J. Humenny, S. Mitzinger, C. B. Khadka, B. K. Najafabadi, I. Vieira and J. F. Corrigan, *Dalton Trans.*, 2012, **41**, 4413; (*d*) R. W. Alder, M. E. Blake, L. Chaker, J. N. Harvey, F. Paolini and J. Schütz, *Angew. Chem., Int. Ed.*, 2004, **43**, 5896; (*e*) J. Messelberger, M. Kumar, S. J. Goodner and D. Munz, *Org. Chem. Front.*, 2021, **8**, 6663.

15 A. Inayeh, R. R. K. Groome, I. Singh, A. J. Veinot, F. C. de Lima, R. H. Miwa, C. M. Crudden and A. B. McLean, *Nat. Commun.*, 2021, **12**, 4034.

16 (*a*) M. Fèvre, P. Coupillaud, K. Miqueu, J.-M. Sotiropoulos, J. Vignolle and D. Taton, *J. Org. Chem.*, 2012, **77**, 10135; (*b*) M. Fèvre, J. Pinaud, A. Leteneur, Y. Gnanou, J. Vignolle, D. Taton, K. Miqueu and J.-M. Sotiropoulos, *J. Am. Chem. Soc.*, 2012, **134**, 6776.